Wisotzky E, Fast M F, Koenig T, Oelfke U and Nill S

Image quality and dose measurements for a new exposure-modulated linac-based kV cone-beam CT device

Purpose:

We analyzed the image quality of a prototype linear accelerator (linac) based Siemens kilovoltage (kV) cone-beam computed tomography (CBCT) scanner by acquiring images of different-sized quality assurance phantoms. This prototype device introduces the concept of automatic exposure modulation (a technique pioneered for conventional CT scanners) to linac based CBCT imaging. The 'Customer Use Test' will bring this prototype to its final state. The image quality of the reconstructed images is compared in terms of image uniformity, signal-to-noise ratio (SNR), contrast-to-noise ratio (CNR), and pre-sampling modulation transfer function (MTF) for a wide range of clinically relevant dose settings. For an asymmetrical body phantom, special emphasis is put on the impact of exposure modulation on the image quality.

Materials and Methods:

Imaging system:

The CBCT system used for this study consists of a Siemens F80 x-ray generator, an Optitop 150/40/80 HC x-ray tube and a PerkinElmer XRD 41 x 41 cm^2 flat-panel imager. The imaging detector is equipped with a highly-efficient CsI phosphor screen and an anti-scatter grid made from lead lamellas and carbon-fibre interspacing material. The source-to-axis distance and the source-to-detector distance are 100.0 cm and 143.2 cm.

CBCT scans can be acquired as 'high quality' (HQ, 360°, two frames per degree) or 'economical' (ECO, 360°, one frame per degree) 'full' scans. Additionally, short scan (200°) and extended field-of-view (eFOV) scan protocols are available. While full and shorts scans have a reconstructed FOV of Ø 26.5 cm x 26.5 cm, the reconstructed eFOV is Ø 46.8 cm x 27.5 cm. A reconstruction matrix size of 512 x 512 voxels was chosen, resulting in a voxel size of 0.56 mm and 0.99 mm respectively. Two slices were binned together for the evaluation. The x-ray generator voltage was set to 121 kVp for all scans. KV CBCT scans, which are normally prone to high levels of scatter artefacts, were corrected using an iterative scatter correction algorithm (Maltz et al 2008) that calculates water-equivalent attenuation lengths and uses pre-calculated scatter kernels to estimate the scatter contribution to the detector signal. The algorithm subsequently performs a beam hardening correction. A smoothing filter was used for the filtered back-projection unless otherwise noted.

The exposure modulation adjusts the current-time-product (mAs) according to the signal level that has been measured at a certain area of the detector. During rotation of the gantry, subsequent frames are analysed and the mAs-value is adapted if necessary to maintain the same signal on the flat-panel detector (target value). A pre-shot image is acquired immediately before the CBCT acquisition (mostly using 0.5 mAs) and the actual and target pixel counts are compared. The system then automatically sets the start mAs for the CBCT acquisition based on user-defined organ programs. While the exposure modulation is enabled by default, we were able to disable it in research mode for the purpose of this study.

Image Quality Phantoms:

To analyze the image quality two commercial phantoms (Catphan 600, ConeBeam Phantom) and an in-house developed Perspex body phantom are used.

The Catphan 600 is an image quality phantom produced by The Phantom Laboratory. The phantom consists of a 20 cm housing, in which five modules of 16 cm diameter are embedded. The different modules serve different imaging purposes. We have selected two modules for evaluation: (a) the CTP 404 module is used to evaluate the high contrast resolution of the CBCT device; it is 25 mm wide and contains seven different contrast materials: air, PMP ($C_6H_{12}(CH_2)$), LDPE (C_2H_4), polystyrene, acrylic, delrin, Teflon; (b) the CTP 486 module is used to measure the uniformity of the different imaging protocols. It is manufactured from water-equivalent compounds; it is 40 mm wide, and free of any high or low density components to avoid adverse effects caused by scatter and beam hardening.

The ConeBeam Phantom is an image quality phantom manufactured by QRM. It has a cylindrical shape and a diameter of 16 cm. This makes it ideal for simulations of head and neck imaging. The phantom includes six different 2 cm thick modules, four of which were used in this study: three low contrast modules and one MTF module. The three low contrast modules were used to evaluate the low contrast resolution of the imaging protocols. Each module has the same layout. It consists of four large and several smaller rods of material with different density. Every rod has a thickness of 16 mm. The MTF module contains a metallic wedge that shows very high contrast to the phantom material and is used to quantify the spatial resolution.

The Perspex ellipse-shaped body phantom is an in-house build image quality phantom. It has two removable inner parts and eight holes for inserts. The circular inner part has five holes for inserts and can be positioned either at a central location (used for our measurement) or on the right hand side of the phantom. The sixth hole is on the left, the seventh at 12 o'clock and the last one at 6 o'clock. In these holes, rods with different electron density are inserted. The dimensions of the phantom are 45 cm for the semi-major axis, the semi-minor axis is 25 cm and the thickness is 10 cm. The eight rod materials are in order of electron density (g/cm^{-3}): air (0), LN-450 (0.4), adipose (0.92), breast (0.99), water (1.0), brain (1.05), CB-2 30% (1.34) and cortical bone (1.82).

Dose measurements:

All dose measurements were performed using the PTW CTDI head (16 cm diameter) and CTDI body (32 cm diameter) phantom. The phantom is an acrylic cylinder with a height of 15 cm and boreholes stretching along the central axes. Measurements of the central dose *DC* and peripheral dose *DP* (summed over all gantry angles) were combined to calculate the weighted central slice CT dose index:

$$CTDI_w = \frac{1}{3}\sum_{all\,angles}(DC) + \frac{2}{3}\sum_{all\,angles}(DP).$$

$CTDI_w$ is a popular surrogate for the *imaging dose* in kV CBCT (Amer *et al* 2007). Due to their similar diameter, the dose values measured with the PTW CTDI head phantom were assumed to be valid for the ConeBeam Phantom and the Catphan

600 phantom; the values measured with the PTW CTDI body phantom were used for the Perspex ellipse-shaped body phantom.

Image quality parameters:

We selected uniformity, signal-to-noise ratio (SNR), and contrast-to-noise ratio (CNR) as image quality parameters:

$$SNR = \frac{CTm}{\sigma_{ROI}}, \quad CNR = \frac{|CTm_{ROI1} - CTm_{ROI2}|}{\sqrt{\sigma_{ROI1}^2 + \sigma_{ROI2}^2}}.$$

Here, the mean CT number of a region of interest (ROI) is abbreviated as CTm. The standard deviation of the CT number within a ROI is denoted as σ. The CNR is calculated by defining appropriate sample ROIs and neighbouring reference ROIs (for small phantoms) or a reference ROI in the water insert (body phantom). For the uniformity, horizontal and vertical CT number profiles were evaluated.

The presampling MTF was measured by oversampling the edge-spread function of the MTF module (ConeBeam phantom) and employing an analytical fit model proposed by Boone & Seibert (1994). The method used for evaluating the MTF is described in greater detail in Fast et al (2012). For this study, 'full' scans with the ECO and HQ dose protocols were analyzed. Statistical significance was achieved by looking at various reconstructed slices and using the bootstrapping method outlined in Fast et al (2012). The edge-preserving filter was used for reconstruction.

Results:

Imaging dose:

We have established a piece-wise linear relationship between current-time-product (mAs) and imaging dose ($CDTI_w$) see table 1. Small non-linearities occur only at extremely low imaging doses. The calculate $CTDI_w$ values for the different protocols are listed in table 2. The total exposure and dose values measured for the different phantoms and protocols used to evaluate the image quality are summarized in table 3.

Table 1: The dose measured at the central position using the CTDI head phantom for a full scan protocol with 377 projections and exposure modulation turned off.

Protocol	Exposure per projection [mAs]	Total exposure [mAs]	Dose [mGy]
ECO full 1	0.5	185.5	5.16
ECO full 2	1.0	396.9	14.74
ECO full 3	2.0	788.0	32.53
ECO full 4	3.0	1410.0	71.57

Table 2: $CTDI_w$ values for the two CTDI phantoms and the available scan modes.

Scan mode	CTDI Phantom	Projections	Total exposure [mAs]	$CDTI_w$ [mGy]
Full	Head	377	396.9	16.75
	Body	721	758.1	26.84
Short	Head	210	105.0	3.11
	Body	401	422.1	11.67
Extended FOV	Body	721	757.2	18.80

Table 3: Total exposure values and corresponding $CTDI_w$ doses for the selected protocols

Phantom	Protocol	Exposure modulation	Total exposure [mAs]	$CTDI_w$ [mGy]
CatPhan	ECO short	Yes	130.3	3.86
	ECO full	Yes	227.0	9.58
	HQ full	Yes	383.1	16.16
	HQ full	No	375.5	15.84
ConeBeam	ECO short	Yes	99.0	2.93
	ECO full	Yes	166.5	7.02
	HQ full	Yes	332.2	14.01
	ECO short	No	105.0	3.11
Body	ECO eFOV	No	1187.1	29.47
	ECO eFOV	Yes	1179.1	29.28
	HQ eFOV	No	2404.2	59.69
	HQ eFOV	Yes	2057.4	51.08

CNR & SNR (small phantoms):

Our study has shown that for circular phantoms there is as expected no significant difference between the CNR of exposure modulated protocols and protocols without exposure modulation.

For the Catphan phantom, the CNR results of the four evaluated protocols are shown in figure 1. The CNR is slightly increased for the protocol using exposure modulation compared to the non-modulated protocol due to a slightly higher $CTDI_w$ value.

Figure 2 shows the same evaluation of the CNR for the ConeBeam phantom. CNR values observed in this study are comparable to values published by Cheng et al (2011) for a Varian OBI 1.4 system and to values published by Kamath et al (2010) for a Varian OBI 1.4 system and an Elekta XVI 4.0 system.

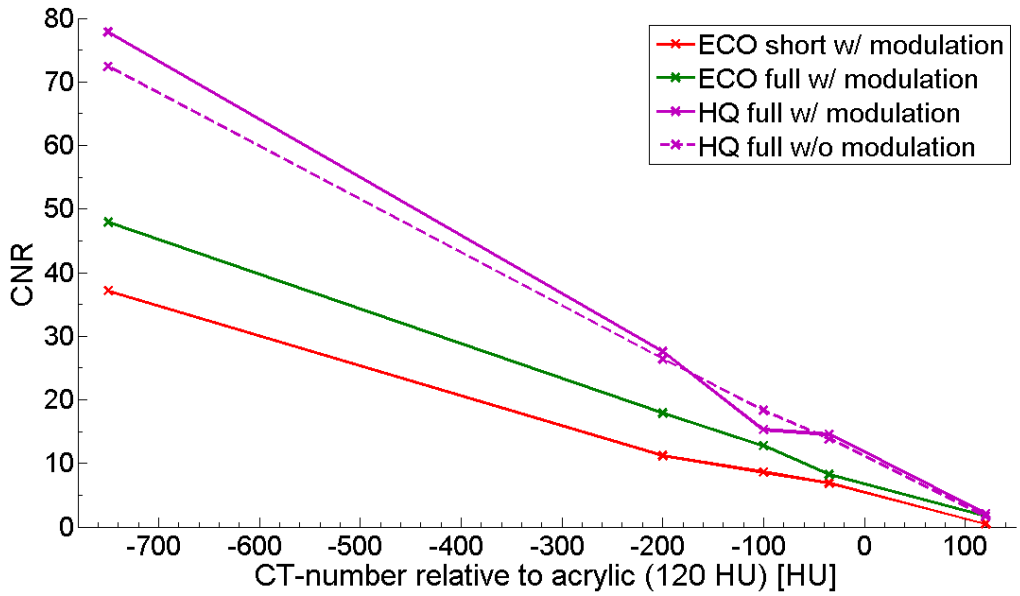

Figure 1: CNR values of the Catphan 600 phantom for the protocols listed in table 3.

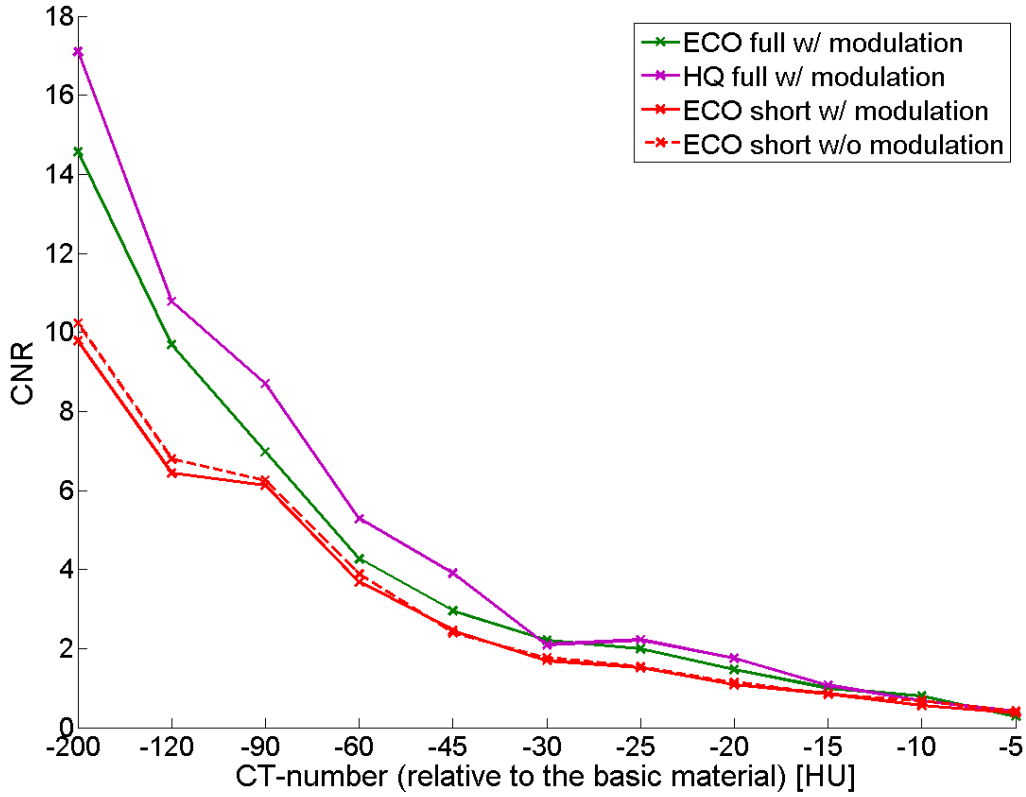

Figure 2: CNR values of the ConeBeam phantom for the protocols listed in table 3.

Uniformity (Catphan 600):

When looking at the overall uniformity of the circular Catphan 600 phantom for different scan protocols, no difference between exposure modulation protocols and the ones without exposure modulation can be observed (see figure 3). Additionally, no significant differences in uniformity between a short and full scan exists. For the eFOV, the uniformity drops for all protocols at the centre of the phantom possibly due to insufficiently corrected beam hardening (not shown).

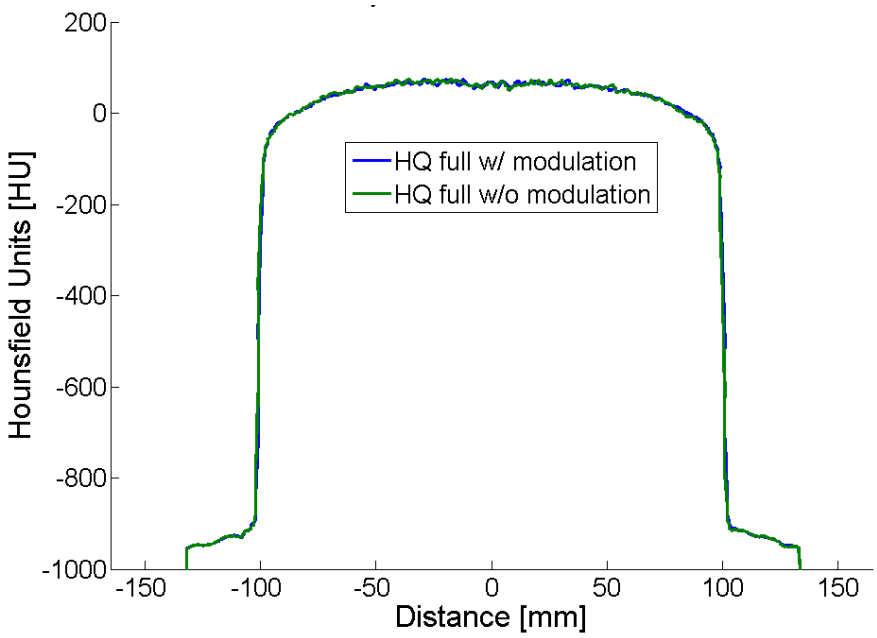

Figure 3: Horizontal profile of the water module of the Catphan 600.

CNR (body phantom):

For the large body phantom, we did observe a small increase in CNR for the modulated protocols (figure 4). The improvement in CNR from going from an ECO protocol to a HQ protocol was modest. In terms of uniformity, we observed that the exposure modulation does result in fewer streaks for low-density objects (air, lung) and also increases the uniformity at the phantom centre.

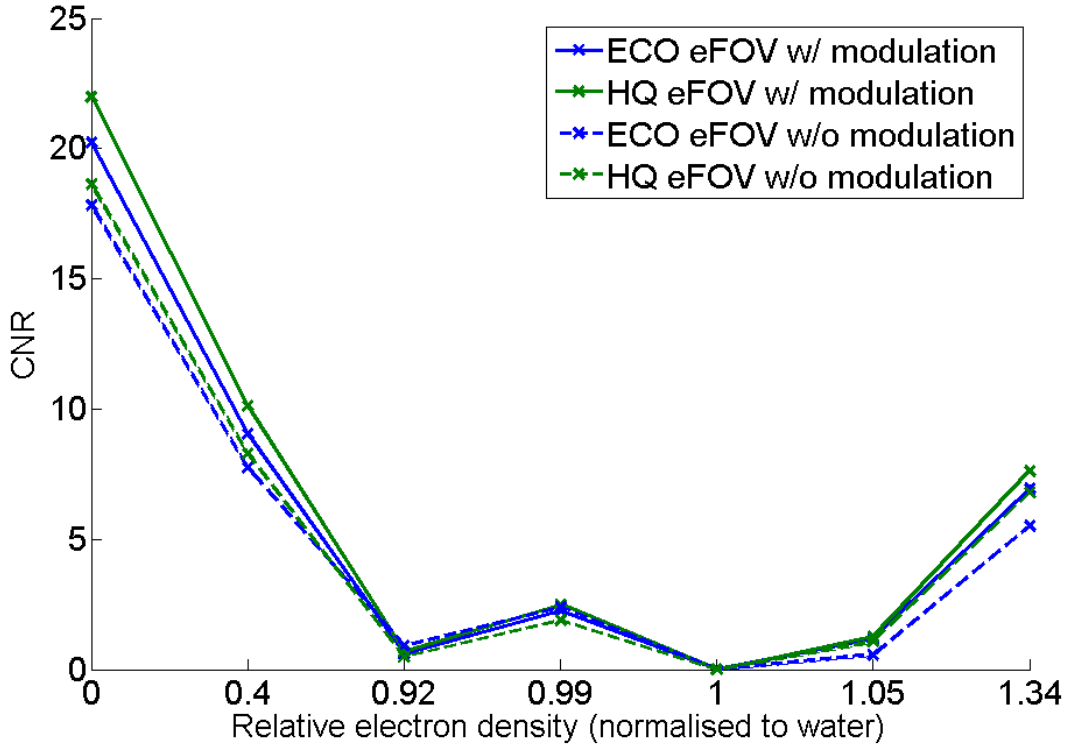

Figure 4: The CNR of the body Perspex phantom. Note that the 'HQ eFOV w/ modulation' scan used approx. 20% less dose than the 'HQ eFOV w/o modulation' scan (table 3).

Spatial Resolution:

In terms of spatial frequency, the experimental evaluation of the MTF slice of the ConeBeam phantom has yielded median values of 0.39/0.41 for MTF_{50} and 0.76/0.79 for MTF_{10} for the HQ full/ECO full protocols. The median MTF value and its 95% confidence interval are shown in figure 5. The measured MTF values are thus significantly better for the MTF_{50} than values reported by Fast et al (2012) with an earlier prototype of this kV CBCT device.

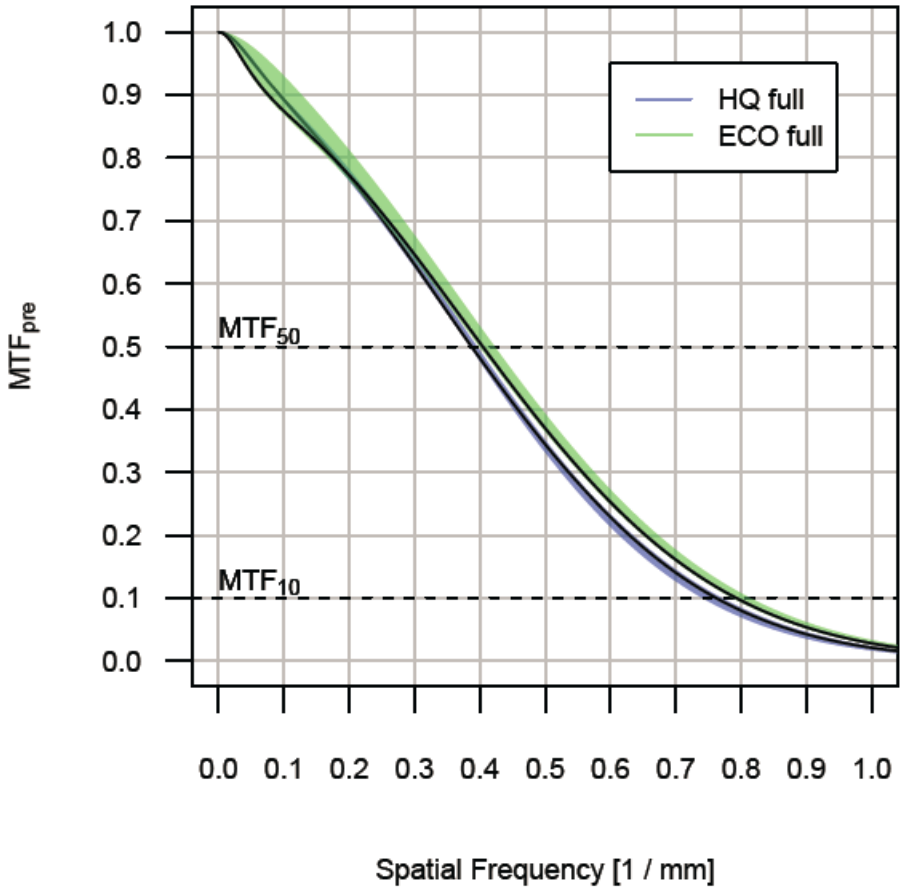

Figure 5: The pre-sampling modulation transfer function (MTF) as function of spatial frequency.

Conclusion:

In this study, we have reported on the image quality of a prototype kV CBCT device with additional exposure modulation capabilities. While the exposure modulation did not impact the image quality of the circular phantoms, an increase in uniformity and CNR, as well as a reduction in streak artifacts could be observed for a larger asymmetrical body phantom. Further evaluation is clearly needed, to identify imaging sites and patient geometries that would benefit most from exposure modulation.

References:

Amer et al (2007), Imaging doses from the Elekta Synergy x-ray cone beam CT system; Brit. J. Radiol. 80.

Boone & Seibert (1994), An analytical edge spread function model for computer fitting and subsequent calculation of the LSF and MTF; Med. Phys. 21.

Cheng et al (2011), Evaluation of radiation dose and image quality for the Varian cone beam computed tomography system; Int. J. Radiat. Oncol. Biol. Phys. 80.

Fast et al (2012), Performance characteristics of a novel megavoltage cone-beam-computed tomography device; Phys. Med. Biol. 57.

Kamath et al (2010), An image quality comparison study between XVI and OBI CBCT systems; J. Appl. Clin. Med. Phys. 12.

Maltz et al (2008), Algorithm for x-ray scatter, beam-hardening, and beam profile correction in diagnostic (kilovoltage) and treatment (megavoltage) cone beam; CT IEEE Trans. Med. Imaging 27.

Conflict of Interest: Supported by Siemens Healthcare/CR.